International Journal of Legal Medicine (2023) 137:329–344
https://doi.org/10.1007/s00414-022-02934-7

ORIGINAL ARTICLE

Multimethod combination for age estimation of *Sarcophaga peregrina* (Diptera: Sarcophagidae) with implications for estimation of the postmortem interval

Yanjie Shang[1] · Jens Amendt[2] · Yu Wang[3] · Lipin Ren[1] · Fengqin Yang[1] · Xiangyan Zhang[1] · Changquan Zhang[1] · Yadong Guo[1]

Received: 11 June 2022 / Accepted: 7 December 2022 / Published online: 20 December 2022

Abstract

Sarcophaga peregrina (Robineau-Desvoidy, 1830) (Diptera: Sarcophagidae) is a forensically important flesh fly with potential value for estimating the minimum postmortem interval (PMI_{min}). Here, the developmental patterns of *S. peregrina* were investigated at 5 constant temperatures (15–35 °C). Morphological changes at different developmental stages of the pupa were observed at 4 constant temperatures (15–30 °C) by removing the puparium and staining the pupa with hematoxylin and eosin. Furthermore, differentially expressed genes (DEGs) were analyzed at 25 °C in the intrapuparial period to estimate the age of *S. peregrina* during the intrapuparial stage. *S. peregrina* completed development from larviposition to adult eclosion at 15 °C, 20 °C, 25 °C, and 30 °C; the developmental durations were 1090.3 ± 30.6 h, 566.6 ± 21.9 h, 404.6 ± 13.01 h, and 280.3 ± 4.5 h, respectively, while the development could not be completed at 35 °C. The intrapuparial period of *S. peregrina* was divided into 12 sub-stages on the basis of the overall external morphological changes; 6 sub-stages on the basis of individual morphological structures such as the compound eyes, antennae, thorax, legs, wings, and abdomen; and 10 sub-stages on the basis of internal morphological changes detected using histological analysis. The period of each sub-stage or structure that appeared was determined. Moreover, we found that 6 genes (*NDUFS2*, *CPAMD8*, *NDUFV2*, *Hsp27*, *Hsp23*, and *TPP*) with differential expression can be used for the precise age estimation of *S. peregrina* during the intrapuparial period. This study provided basic developmental data for the use of *S. peregrina* in PMI_{min} estimation, and we successfully estimated PMI_{min} in a real forensic case by using a multimethod combination.

Keywords Forensic entomology · Postmortem interval · Flesh fly intrapuparial development · Histological analysis · Differentially expressed genes

Introduction

The minimum postmortem interval (PMI_{min}) can be crucial evidence in criminal cases, and entomological evidence provides new entry points and clues for its estimation [1]. Forensic entomologists can calculate PMI_{min} on the basis of the developmental stage and age of necrophagous insects developing on a corpse [2]. Therefore, it is particularly important to collect accurate basic developmental data of forensically important species [3].

Flesh flies are important necrophagous taxa, as they usually appear on corpses slightly later than the first colonizers, the blow flies [4]. They are sometimes part of the dominant fauna in indoor crime scenes, and they may be the first species to arrive on carrion in rainy seasons [5, 6]. Many studies have reported the existence of flesh flies on human

✉ Changquan Zhang
zcq1105@163.com

✉ Yadong Guo
gdy82@126.com

[1] Department of Forensic Science, School of Basic Medical Sciences, Central South University, Changsha 410013, Hunan, China

[2] Institute of Legal Medicine, University Hospital Frankfurt, Goethe-University, Kennedyallee 104, 60596 Frankfurt am Main, Germany

[3] Department of Forensic Medicine, Soochow University, Ganjiang East Road, Suzhou 215000, China

corpses or animal carcasses worldwide [7]. Basic developmental data from different regions have been established for some flesh fly species such as *Parasarcophaga similis* (Meade 1876) [8], *Sarcophaga (Liosarcophaga) dux* (Thomson, 1869) [9], and *Sarcophaga ruficornis* (Fabricius, 1794) [10]. Several developmental models, such as isomorphen/isomegalen diagrams and thermal summation models, have been used to estimate the age of the immature stages [11].

The intrapuparial period of a fly is an important stage in its metamorphosis, accounting for about half of the total developmental time of the immature stage [12]. Pupal age is difficult to estimate, as the pupa is hidden inside the non-transparent puparium. Many methods and technologies have been used to estimate the age of flies during the intrapuparial stage, for example, optical coherence tomography [13], microcomputed tomography [14], and hyperspectral imaging [15]. Examination of morphological changes during metamorphosis is economical and easy, as the puparium is removed and examined under a stereomicroscope. To date, the intrapuparial development of forensically important fly species, such as *Calliphora grahami* (Aldrich, 1930) [16], *Lucilia illustris* (Meigen, 1826) [17], and *Chrysomya albiceps* (Wiedemann, 1819) [18], has been studied. Subsequent histological analysis of fly pupae can provide further information, allowing for accurate age estimation. Additionally, analysis of differentially expressed genes (DEGs) represents a potential method to estimate the age of flies during the intrapuparial stage, e.g., for the forensically important blow flies *Lucilia sericata* (Meigen, 1826) [19, 20], *Calliphora vicina* (Robineau-Desvoidy, 1830) [21], and *Lucilia illustris* (Meigen, 1826) [17] and the flesh fly *Sarcophaga dux* (Thomson, 1869) [9]. A combination of the more challenging gene expression method and the analysis of internal and external metamorphosis of the pupa would generate a more precise PMI_{min}.

The flesh fly *Sarcophaga peregrina* (Robineau-Desvoidy, 1830) (Diptera: Sarcophagidae) is an important species in the medical, veterinary, and forensic entomology fields [22]. Geographically, this species is widely distributed in the Palaearctic, Oriental, and Australasian regions [23]. The presence of *S. peregrina* has been proven in many insect succession studies as well as on human bodies [24, 25]. Wang et al. (2017) investigated the development of *S. peregrina* at constant temperatures [26]; however, many studies have discussed the developmental plasticity of flies and argue that different populations may reveal differences in development [27]. Furthermore, differences in experimental designs or feeding substrates may lead to discrepancies in the reported developmental time [28].

In this study, *S. peregrina* larvae from Hunan Province, China, were reared using fresh pig lungs to establish a laboratory population. Subsequently, the basic developmental data of *S. peregrina* were established at 5 constant temperatures, using different temperature settings than those reported in previous studies. Then, external morphological and internal histological changes during the intrapuparial period of *S. peregrina* were described. In addition, the expression profiles of 6 DEGs (*NDUFS2*, *CPAMD8*, *NDUFV2*, *Hsp27*, *Hsp23*, and *TPP*) of *S. peregrina* during the intrapuparial period at 25 °C were obtained.

This study provides additional developmental data for the use of *S. peregrina* in forensic entomology. We proved the applicability of these data by reporting a forensic case in which the development of *S. peregrina* was used to estimate PMI_{min}.

Material and methods

Establishment of laboratory populations

In July 2020, insect colonies were established from adult specimens of *S. peregrina* baited using pig lungs in Changsha City (28°12′N, 112°58′E), Hunan Province, China. Species identification was performed on the basis of morphology, according to the identification key of Chen [29]. The adults were maintained in an insect cage (35 cm × 35 cm × 35 cm) with natural illumination and temperature and 75% humidity. The adults were fed a combination of milk powder and white sugar (1:1). The water supply of the flies was ensured using a culture dish and regularly moistened cotton. A 10-cm culture dish containing 20 g of fresh pig lung was placed in the rearing cages to induce larviposition. The resulting larvae were reared on fresh pig lung ad libitum. The colonies were maintained for 5 generations, with the number of adults between 1000 and 3000, before the start of the study.

Monitoring of developmental duration and measurement of larval body length

A 10-cm culture plate with 2 g of pig lung was placed in the insect-rearing cage to induce larviposition. The resulting larvae (ca. 1,500) produced within 1 h were separated into 5 groups of approximately 300 larvae each and placed in 5 rearing boxes (17 cm × 12 cm × 8 cm) with sawdust at the bottom. At the start of the experiment, 100 g of pig lung was provided in each rearing box. The rearing boxes were placed in climate boxes (LRH-250-GSI; Taihong Co., Ltd, Shaoguan, China) at constant temperatures of 15 °C, 20 °C, 25 °C, 30 °C, and 35 °C and 75% humidity and a photoperiod of 12:12 h (L:D). Fresh pig lung was supplied regularly ad libitum to meet the nutritional needs of the larvae until pupation.

The larvae were sampled every 8 h; at each inspection time, 10 larvae were randomly selected from 5 rearing

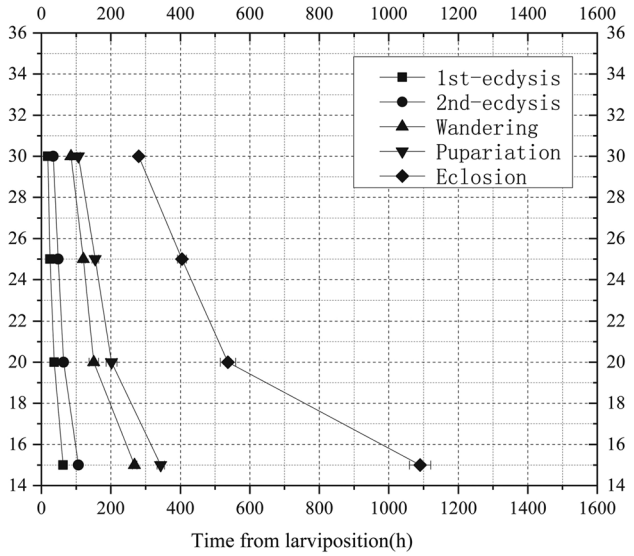

Fig. 1 Isomorphen diagram of *Sarcophaga peregrina*. The duration of each development milestone (first ecdysis, second ecdysis, wandering, pupation, and eclosion) was plotted with the time from larviposition to the onset of each milestone. Each curve corresponds to a developmental milestone, and the error bar is the standard deviation of each milestone

boxes and immersed in 80 °C hot water for 30 s before being preserved in 80% ethanol [30]. After storage for 24 h, the sampled larvae were examined with a Zeiss 2000-C stereomicroscope (Carl Zeiss, Germany), and instars were determined on the basis of the number of posterior spiracles. The length of each larva was measured with a digital caliper (Mineette, Shanghai, China) [31]. When approximately 50% post-feeding larvae were observed to form puparia, samples were not collected until eclosion. During the experiment, each developmental event, including the first, second, and third instar, wandering, pupation, and eclosion, was defined when approximately 50% of individuals from the previous stage reached the next stage of development, and the times of each development event were recorded. Three replicates were performed at each temperature in different incubators.

Observation of external morphological changes

The larvae generated within 1 h were cultured in a rearing box at 15 °C, 20 °C, 25 °C, and 30 °C, 75% humidity, and 12:12 h light/dark cycle (see above). When approximately 50% of the post-feeding larvae formed white puparia, the first sample was collected. Ten pupae were sampled every 8 h until adult eclosion [17]. The pupae were fixed in 80 °C hot water for 30 s and then stored in 80% ethanol. Each experiment was repeated 3 times in different incubators at each temperature. Pupal development lasted approximately 33 days at 15 °C, 16 days at 20 °C, 10 days at 25 °C, and 7 days at 30 °C. A total of 5940 pupae were collected: 2970 pupae at 15 °C, 1440 pupae at 20 °C, 900 pupae at 25 °C, and 630 pupae at 30 °C.

After a week of storage, the puparium was carefully removed with insect needles, forceps, and ophthalmic scissors, and morphological changes of the pupae were observed and imaged with a Zeiss Stemi_508 stereomicroscope and Axiocam 208 microcamera (Carl Zeiss, Germany).

Observation of internal histological changes

Larviposition and larval rearing were performed using the methods described previously. After pupariation, 10 pupae were collected every 8 h under 4 different constant temperature conditions of 15 °C, 20 °C, 25 °C, and 30 °C until eclosion. Each experiment was repeated 3 times in different incubators at each temperature.

All samples were killed in 80 °C hot water for 30 s, and the puparium was carefully removed using the method described previously. All pre-processed samples, including the needled pupae and intrapuparial tissue of the removed puparium, were preserved in 80% ethanol for 1 week at 4 °C, immersed in Carnoy's preservative for 24 h at 4 °C, and transferred into 10% formaldehyde solution for 12 h at room temperature before histological processing. Subsequently, dehydration, paraffin infiltration, embedding, sectioning, and hematoxylin–eosin (HE) staining were performed [32]. In particular, the maximum longitudinal section of each sample was used for sectioning and staining. All HE slides of the pupae were scanned and electronically preserved using the Motic automatic digital slice scanning and application system (Motic, USA). The internal histological changes of the puparia were observed and recorded using the supporting software Motic DSAssistant Lite VM V1 2.0 (Motic, USA).

Table 1 Mean (±SD) development duration (h) of *S. peregrina* at four constant temperatures

Developmental stages	First instar	Second instar	Third instar	Wandering	Pupariation	Total duration
15℃	62.6±2.3	44.3±4.04	161.3±6.1	75.3±4.1	746.6±28.09	1090.3±30.6
20℃	36.6±5.03	27.3±4.1	86.6±6.1	51.3±4.1	364.6±8.3	566.6±21.9
25℃	24.6±3.05	23.6±1.5	72.6±3.05	34.3±4.9	249.3±8.3	404.6±13.01
30℃	18.3±4.9	15.6±1.5	51.3±3.05	21.6±2.5	173.3±6.1	280.3±4.5

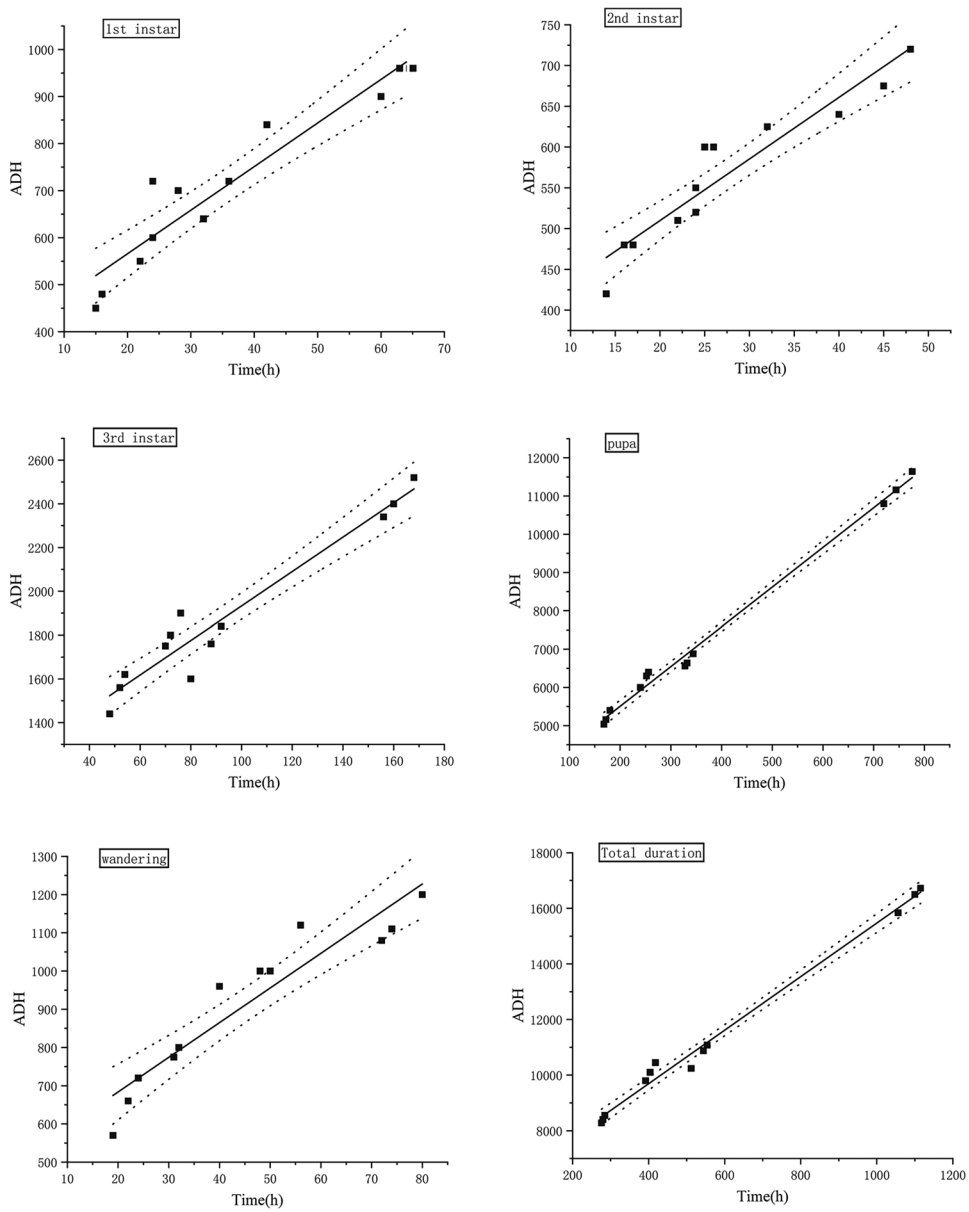

Fig. 2 Thermal summation models for five developmental stages and total development duration of *Sarcophaga peregrina*. The solid line represents the regression line, and the dashed line represents 95% confidence interval

Table 2 Mean (±SE) of developmental threshold temperatures (D_0) and thermal summation constants (K) for five developmental stages and the total development period of *S. peregrina* and the coefficient of determination (R^2) of thermal summation models

Developmental stages	K (degree hours)		D_0 (°C)		R^2
	Mean	SE	Mean	SE	
1st instar	380.27794	38.39906	9.26619	0.97073	0.90111
2nd instar	358.74873	24.09981	7.5526	0.80969	0.89692
3rd instar	1145.24369	65.54686	7.87372	0.64338	0.93741
wandering	502.09594	50.20531	9.06907	1.00401	0.89082
pupa	3431.34915	110.8142	10.37318	0.25383	0.99405
Total duration	5836.7749	189.79503	9.63144	0.28941	0.99105

Differential gene expression analysis

The above-mentioned method was used to induce larviposition and larval rearing at a constant temperature of 25 °C. After pupation, the intrapuparial age of *S. peregrina* was set to "zero" when approximately 50% of the post-feeding larvae formed puparia, and 10 pupae were collected every 48 h until eclosion. The experiment was repeated 3 times

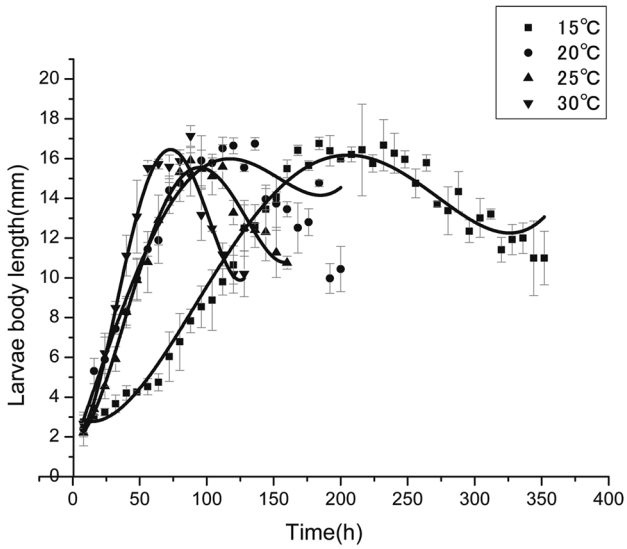

Fig. 3 Changes in *Sarcophaga peregrina* larval body length (mm) over time (h) at different constant temperatures. The vertical bars represent the standard deviation

in different incubators at 25 °C. A total of 150 pupae were collected. All samples were collected in a 5 ml cryovial and frozen immediately in liquid nitrogen and stored at − 80 °C.

The total RNA of intrapuparial tissues of *S. peregrina* was isolated using the Steady Pure Universal RNA Extraction Kit (Code No. AG21017; Accurate Biotechnology Co., Ltd, Hunan, China), according to the manufacturer's instructions. The total RNA was quantified with the NanoDrop™ 2000 Spectrophotometer (Thermo Fisher Scientific). The first-strand cDNA was synthesized from the total RNA (10 ng to 5 µg) by using the Evo M-MLV RT Mix Kit with gDNA Clean for qPCR (Code No. AG11728; Accurate Biotechnology Co., Ltd, Hunan, China), according to the manufacturer's instructions.

Candidate differentially expressed genes (DEGs) were selected from the reference genome [33] (NCBI no. JABZEU000000000) and transcriptome data (NCBI no. PRJNA795032) of *S. peregrina*. Quantitative real-time PCR was performed using the SYBR® Green Premix Pro Taq HS qPCR Kit (ROX Plus, Code No. AG11718; Accurate Biotechnology Co., Ltd, Hunan, China), according to the manufacturer's instructions on an ABI 7500 Real-Time PCR system (Applied Biosystem, Carlsbad, CA, USA). Primers for the DEGs and internal control genes were designed using Primer 5.0 software (Biosoft Premier, Palo Alto, California, USA). The actin gene was used as the internal control for qPCR. All primers are listed in Table S1.

Statistical analysis

An isomorphen diagram of the time (*x*-axis) taken to reach distinct developmental events at different constant temperatures (*y*-axis) was created. In this study, the revised linear regression model suggested by Ikemoto and Takai (2000) [9] was used to perform linear regression analysis of the connection between developmental time and accumulated degree hours (ADH) at various stages of development. The slope and intercept of the linear regression equation were used to calculate the development threshold temperature (D_0) and thermal summation constant (K) [34]. The association between larval body length and time after larviposition was investigated to develop a simulation equation for PMI_{min} estimation by using polynomial regression analysis.

The relative expression levels of DEGs at different intrapuparial ages of *S. peregrina* were quantified using the $2^{-\Delta\Delta Ct}$ method. The log-transform to the base of 2 [$\log_2$ FC] (fold change, FC, i.e., relative change in gene expression) was used to normalize the values of the DEGs [23]. The connection between DEG expression level and percentage of intrapuparial development of *S. peregrina* was mapped using polynomial regression analysis. The results are shown as mean ± standard deviation (SD) values of 3 biological replicates.

All statistical analyses of the data were conducted using Origin Pro 8.6 software (OriginLab, Northampton, MA, USA, SCR: 015,636) and Prism software (GraphPad Software Inc. La Jolla, CA, USA, SCR: 002,798).

Results

Duration of development and isomorphen diagram

S. peregrina completed its development from larva to adult at temperatures between 15 °C and 30 °C but not

Table 3 Equations, *P* values, degrees of freedom (df), and coefficients of determination (R^2) of the relationship between the body length (L) (mm) of *S. peregrina* larvae and the time after larviposition (T) (h) at four constant temperatures

Temperature (℃)	Equation	df	*P*	R^2
15	$L = 3.10351 - 0.04941\ T + 0.00197T^2 - 9.63738E\text{-}6T^3 + 1.32569E\text{-}8T^4$	39	< 0.001	0.996
20	$L = 1.34071 + 0.18656\ T + 6.29557E\text{-}4T^2 - 1.50825E\text{-}5T^3 + 4.46068E\text{-}8T^4$	20	< 0.001	0.90521
25	$L = 1.92631 - 0.0084\ T + 0.00676T^2 - 7.56699E\text{-}5T^3 + 2.24446E\text{-}7T^4$	15	< 0.001	0.99653
30	$L = 2.43455 - 0.09954\ T + 0.01456T^2 - 1.98607E\text{-}4T^3 + 7.38778E\text{-}7T^4$	11	< 0.001	0.98298

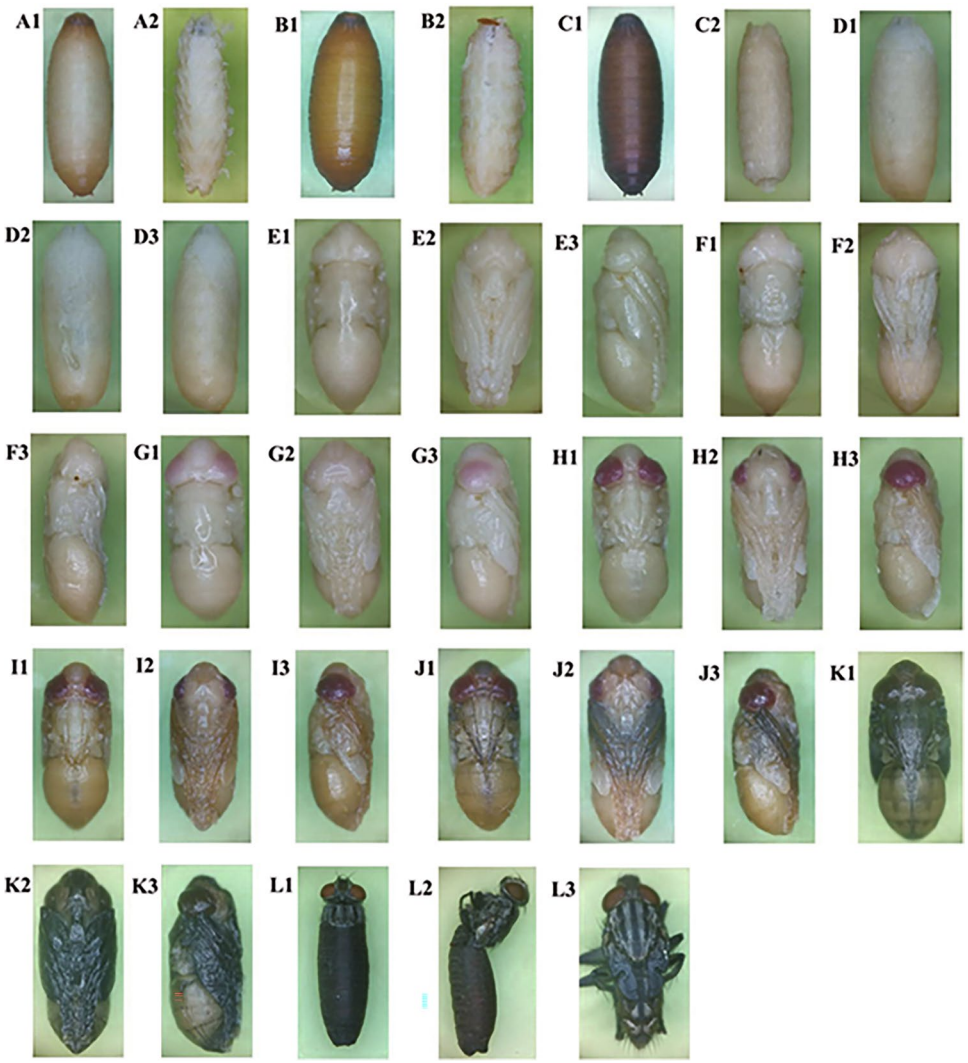

Fig. 4 Intrapuparial morphological changes of *Sarcophaga peregrina*. **A** White pupal stage; **B** yellow pupal stage; **C** early cryptocephalic pupal stage; **D** late cryptocephalic pupal stage; **E** phanerocephalic pupal stage; **F** yellow eye stage; **G** pink eye stage; **H** red eye stage; **I** thorax and abdomen bristle obvious stage; **J** leg and wing pigmentation stage; **K** brown-eyed stage; **L** teneral emergence stage

at 35° C. The total development time decreased as the temperature increased. The total developmental duration was 1090.3 ± 30.6 h at 15 °C and 280.3 ± 4.5 h at 30 °C (Table 1).

The time (*x*-axis) needed for distinct developmental events at different constant temperatures (*y*-axis) was used to create an isomorphen diagram (Fig. 1). The amount of time until each developmental milestone (first ecdysis, second ecdysis, wandering, pupariation, and eclosion) steadily decreased as the temperature increased in the range of 15–30 °C, and the various curve intervals grew shorter as the temperature increased.

Thermal summation model

Six thermal summation models (including the 5 developmental stages, first instar, second instar, third instar, wandering, pupariation, and the total developmental process) were constructed on the basis of the linear regression analysis of the relationship between the developmental time (*x*-axis) and accumulated degree hours ADH (*y*-axis) of each developmental stage and the entire development process (Fig. 2). According to the results calculated by the model, the developmental threshold temperature D_0 and thermal summation constant K of the entire developmental process were 9.6 ± 0.29 °C and 5836.8 ± 189.8 degree hours, respectively (Table 2).

Changes in larval body length

Larval body lengths with time after larviposition at different temperatures are shown in Fig. 3, and the larval development rate increased rapidly as the temperature increased between the range of 15 °C and 30 °C. Table 3 shows the changes in larval body length (L) as a function of time (T), with time after hatching as the independent variable and larval body length as the dependent variable. According to

Table 4 Intrapuparial development of *S. peregrina* related to hours (h) after pupariation at different temperatures

Sub-stage	15℃				20℃				25℃				30℃			
	Min (h)	Max (h)	Mean	SD	Min (h)	Max (h)	Mean	SD	Min (h)	Max (h)	Mean	SD	Min (h)	Max (h)	Mean	SD
A	0	24	13.65	8.12	0	16	9.92	6.11	0	8	5.78	3.58	0	8	3.87	4.00
B	24	48	39.27	11.55	16	32	24.38	7.99	8	16	14.00	3.46	8	16	10.86	3.83
C	48	96	73.85	23.93	32	48	40.96	7.94	16	32	26.67	7.54	16	24	21.71	3.61
D	96	144	111.72	26.20	48	72	59.47	10.05	32	48	40.29	6.92	24	40	32.35	10.52
E	144	240	191.37	33.71	72	96	83.88	9.26	48	80	65.70	11.44	40	72	55.23	11.56
F	240	408	325.28	57.91	96	184	138.96	28.07	80	144	112.00	20.74	72	96	81.49	13.53
G	408	480	443.14	52.08	192	224	207.77	20.92	144	168	155.86	8.82	96	112	104.67	6.90
H	480	528	506.67	19.96	224	240	232.31	6.46	176	184	179.81	4.00	120	136	131.10	6.55
I	528	576	553.71	20.21	248	280	265.18	11.17	184	200	191.72	6.12	136	144	142.10	6.21
J	552	648	599.35	34.62	280	304	292.86	9.40	200	224	212.41	8.56	144	160	155.67	6.72
K	648	744	697.45	33.91	312	360	336.55	16.92	224	240	231.59	8.56	160	168	165.66	6.77
L	744	792	768.83	19.41	360	376	367.71	6.58	240	256	249.17	4.00	168	184	173.31	3.99

the coefficient of determination (R^2) and P value, the regression models showed a good fit for the data [17].

Intrapuparial external morphological changes over time

Overall changes in the morphology of *S. peregrina* were categorized into 12 sub-stages (A–L), according to the previously reported division of intrapuparial phases for different species (Fig. 4) [2]. Table S2 lists the typical features of each sub-stage, and Table 4 shows the time ranges of each sub-stage for the external morphology of *S. peregrina* at various temperatures.

Intrapuparial external morphological changes in a single organ over time

The age of the intrapuparial stage can be determined by the changes in certain morphological traits such as compound eyes, antennae, the entire thorax, legs, wings, and the entire abdomen (Fig. 5). Table 5 shows the time range for each of these structures at various temperatures.

Intrapuparial internal histological changes over time

The internal morphological changes of *S. peregrina* pupae can be divided into 10 sub-stages on the basis of the histological analysis (Fig. 6). HE-stained pupal sections revealed differences in the internal changes in body development throughout the intrapuparial stage, showing the potential for age estimation. The typical characteristics of each sub-stage are listed in Table S3. The time ranges of each sub-stage for internal morphological changes of *S. peregrina* at different temperatures are listed in Table 6.

Overall gene expression profiles during intrapuparial development

The overall expression profiles of the 6 DEGs (*NDUFS2*, *CPAMD8*, *NDUFV2*, *Hsp27*, *Hsp23*, and *TPP*) showed potential developmental-specific and statistical relevance for predicting *S. peregrina* intrapuparial age. Figure 7 shows the overall expression levels of the 6 DEGs at 25 °C plotted against the percentage of intrapuparial development. During pupal development, the expression patterns of *NDUFS2*, *CPAMD8*, and *NDUFV2* increased, whereas those of *Hsp27*, *Hsp23*, and *TPP* decreased.

Polynomial regression analysis was used to create simulation equations for the association between DEG expression levels during *S. peregrina* intrapuparial development and the percentage of intrapuparial development (Table 7).

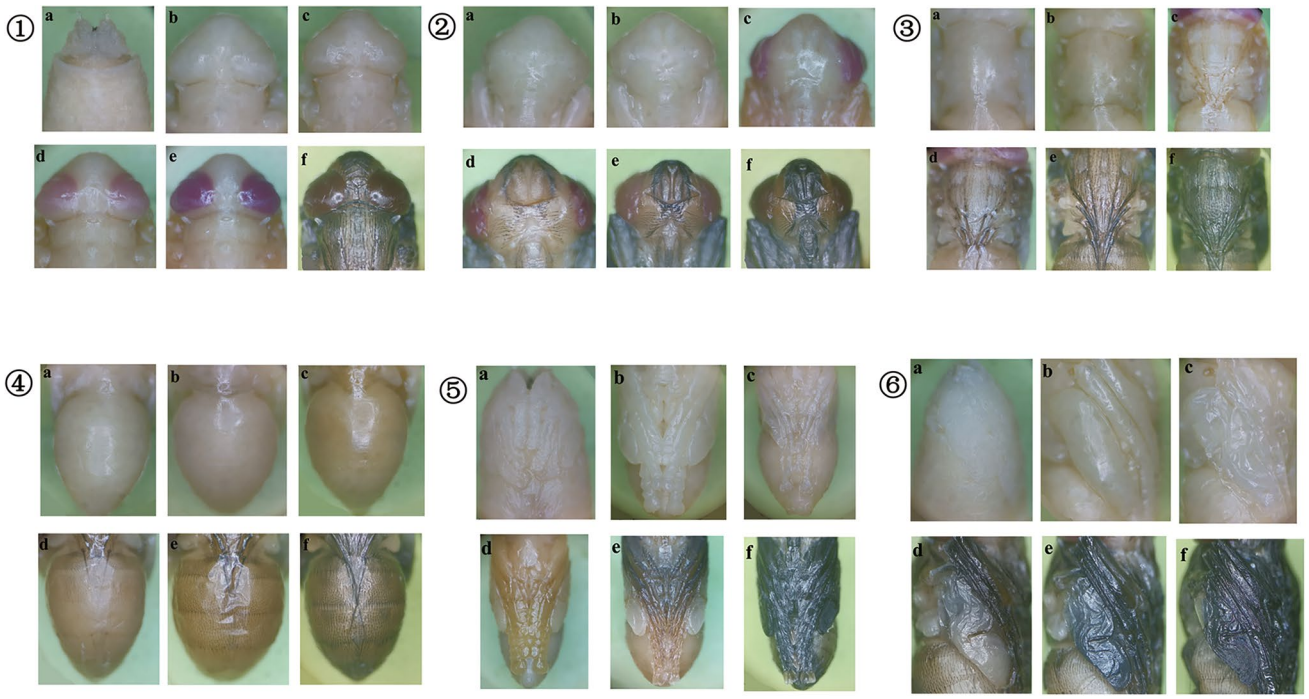

Fig. 5 (**1**) Intrapuparial development of the compound eyes of *Sarcophaga peregrina*. (a) The compound eyes are initially absent; (b) no boundary or no clear boundary between the compound eyes and thorax; (c) clear boundary between the head and thorax; (d) pink compound eyes; (e) red compound eyes; and (f) brown compound eyes. (**2**) Intrapuparial development of the antennae of *Sarcophaga peregrina*. (a) The antennae are initially absent; (b) the antennae initially emerge, but the contour is vague; (c) the antennae have obvious contours; (d) the antennae are light brown; (e) the antennae show further pigmentation and are brown; and (f) fully developed black–brown antennae. (**3**) Intrapuparial development of the thorax of *Sarcophaga peregrina*. (a) No boundary or no clear boundary between the thorax and head/abdomen; (b) clear boundary between the thorax and head/abdomen; (c) light yellow thoracic dorsal bristles; (d) light brown thoracic dorsal bristles; (e) brown–yellow thorax with black–brown thoracic dorsal bristles; and (f) ash black thorax with dark black thoracic dorsal bristles. (**4**) Intrapuparial development of the abdomen of *Sarcophaga peregrina*. (a) no boundary or no clear boundary between the abdomen and thorax; (b) clear boundary between the abdomen and thorax; (c) light yellow abdomen dorsal bristles; (d) yellow–white abdomen with brown hair; (e) brown–yellow abdomen with brown–black hair; and (f) gray–black abdomen with black hair. (**5**) Intrapuparial development of the legs of *Sarcophaga peregrina*. (a) short legs, less than one-third of the pupa; (b) thick and long legs; (c) thinned legs with tarsomeres; (d) light brown legs; (e) dark brown legs; and (f) black legs. (**6**) Intrapuparial development of the wings of *Sarcophaga peregrina*. (a) short and small wings; (b) thick and long wings; (c) thin wings with visible veins;(d) light gray wings; (e) grayish black wings; and (f) black wings

Case report using *S. peregrina* for the estimation of PMI_{min}

At 1300 on May 22, 2020, an anonymous complaint about a foul odor emanating from a rental room led to a police investigation, and the police found a 56-year-old female dead in her rented room. The door was locked from the inside, and there was no trace of forced entry. The body was lying on a small handcart in a supine position, and advanced decomposition was detected with pooled body fluid beneath the body (Fig. 8a). Numerous third instar maggots and light brown to dark brown pupae were found on the corpse and at the death scene, but no empty puparia or dead flies were detected at the scene of the death; the oldest insect samples were the dark brown pupae (Fig. 8b). The police examined the cadaver but did not find any signs of mechanical injury. The toxicology analysis yielded negative results for common toxic drugs. Homicide was excluded after forensic medical examination. The cause of death was considered as sudden death. Insect samples from the corpse and death scene, including pupae, were collected (Fig. 8c), placed in a breathable plastic container, and immediately sent to the Forensic Entomological Laboratory of Central South University within 12 h for estimation of PMI.

The temperature data were collected from the scene of death, surface of the corpse, and maggot masses by using a temperature and humidity data logger. Then, temperature changes over the previous weeks were investigated using the nearest meteorological station, and the corrected temperature average was 25 °C. Puparia were carefully removed from the insect samples (dark brown pupae) with insect needles, forceps, and ophthalmic scissors, and these puparia were used to extract the total DNA for species identification. We identified the species by amplifying and sequencing long

Table 5 Intrapuparial morphological changes of the head, thorax, and abdomen of *S. peregrina* related to hours (h) after pupariation at different temperatures

	Sub-stage	15℃				20℃				25℃				30℃			
		Min	Max	Mean	SD	Min	Max	Mean	SD	Min	Max	Mean	SD	Min	Max	Mean	SD
Compound eyes	a	0	144	76.29	48.02	0	72	42.07	24.79	0	48	23.27	15.98	0	40	20.95	13.40
	b	144	240	190.96	35.01	72	96	84.67	8.62	48	80	65.20	11.67	40	72	56.44	11.77
	c	240	408	325.28	57.91	96	184	138.86	31.29	80	144	110.93	20.83	72	112	91.37	13.57
	d	408	480	443.14	52.08	192	224	208.62	11.93	144	168	155.86	9.31	112	128	118.67	6.39
	e	480	648	561.23	54.11	224	304	264.96	28.29	176	224	201.54	16.16	136	152	149.27	15.98
	f	648	792	721.04	46.13	312	376	345.21	21.59	224	256	243.69	14.25	152	184	172.53	11.47
Antenna	a	0	240	123.89	76.81	0	96	50.72	30.17	0	80	42.05	25.54	0	72	36.47	22.48
	b	240	408	325.28	57.91	96	168	130.44	23.91	80	128	102.52	16.30	72	104	90.18	11.36
	c	384	480	437.33	34.46	168	224	195.13	18.23	128	176	153.14	16.80	104	120	116.57	8.93
	d	480	576	524.57	34.96	224	280	249.03	18.37	184	200	192.67	6.90	120	136	128.07	12.00
	e	576	648	609.60	26.00	280	304	292.71	9.13	200	224	213.54	9.61	136	152	141.71	9.28
	f	648	792	721.04	46.13	312	376	341.75	22.38	224	256	241.82	13.42	152	184	172.53	11.47
Thorax	a	0	240	123.89	76.81	0	96	50.72	30.17	0	80	42.05	25.54	0	72	36.47	22.48
	b	240	480	358.24	79.58	96	224	155.14	39.56	80	168	121.82	28.38	72	120	100.36	17.52
	c	480	528	506.67	19.96	224	240	232.53	6.17	176	184	180.57	3.96	120	136	128.07	12.00
	d	528	576	553.71	20.21	248	280	262.67	11.70	184	200	192.67	6.90	136	144	140.91	6.17
	e	552	648	599.35	34.62	280	304	292.71	9.13	200	224	213.54	9.61	144	152	147.45	6.67
	f	648	792	721.04	46.13	312	376	341.75	22.38	224	256	241.82	13.42	152	184	172.53	11.47
Abdomen	a	0	240	123.89	76.81	0	96	50.72	30.17	0	80	42.05	25.54	0	72	36.47	22.48
	b	240	480	358.24	79.58	96	224	155.14	39.56	80	168	121.82	28.38	72	120	100.36	17.52
	c	480	528	506.67	19.96	224	240	232.53	6.17	176	184	180.57	3.96	120	136	128.07	12.00
	d	504	576	538.50	28.10	232	280	253.54	16.57	184	200	192.67	6.90	136	144	140.91	6.17
	e	552	648	599.35	34.62	280	304	292.71	9.13	200	224	213.54	9.61	144	152	147.45	6.67
	f	648	792	721.04	46.13	304	376	341.75	22.38	224	256	241.82	13.42	152	184	172.53	11.47
Legs	a	96	144	122.18	19.02	48	72	58.29	9.28	32	48	40.62	6.63	24	40	32.73	6.34
	b	144	240	196.24	34.18	72	96	86.12	8.90	48	80	63.11	12.19	40	72	54.22	11.17
	c	240	480	358.24	79.58	96	224	155.14	39.56	80	168	121.82	28.38	72	120	100.36	17.52
	d	480	576	524.57	34.96	224	280	249.03	18.37	176	200	188.57	8.93	128	144	133.07	12.00
	e	552	648	599.35	34.62	280	304	292.71	9.13	200	224	213.54	9.61	144	152	147.45	6.67
	f	648	792	721.04	46.13	304	376	341.75	22.38	224	256	241.82	13.42	152	184	172.53	11.47
Wings	a	96	144	122.18	19.02	48	72	58.29	9.28	32	48	40.62	6.63	24	40	32.73	6.34
	b	144	240	196.24	34.18	72	96	86.12	8.90	48	80	63.11	12.19	40	72	54.22	11.17
	c	240	504	374.09	87.77	96	240	164.29	44.80	80	176	123.53	30.39	72	128	108.11	23.20
	d	528	576	553.71	20.21	248	280	262.67	11.70	184	200	192.67	6.90	136	144	142.91	6.17
	e	552	648	599.35	34.62	280	304	292.71	9.13	200	224	213.54	9.61	144	152	147.45	6.67
	f	648	792	721.04	46.13	304	376	341.75	22.38	224	256	241.82	13.42	152	184	172.53	11.47

cytochrome oxidase subunit I, COI-J-1460, 5′-TACAATTTATCGCCTAAACTTCAGCC-3′ (forward), and COI-N-2800, 5′-CATTTCAAGCTGTGTAAGCATC-3′ (reverse), using published conditions [23]. The obtained sequences were submitted to GenBank and analyzed for sequence similarity to published COI sequences through BLAST analysis against the NCBI nt/nr database. The specimen sequence from the corpse showed the highest consistency with *S. peregrina*, and the Max ident was 99.91%.

Some of the intrapuparial tissue obtained from the puparium was used to observe external morphological changes and internal histological changes with the method described previously, and the rest of the intrapuparial tissue was frozen immediately in liquid nitrogen and later used to extract the total RNA for analyzing the expression of DEGs. According to the basic developmental data established in this study, it would take 155 h (larval development time) for *S. peregrina* to reach pupation

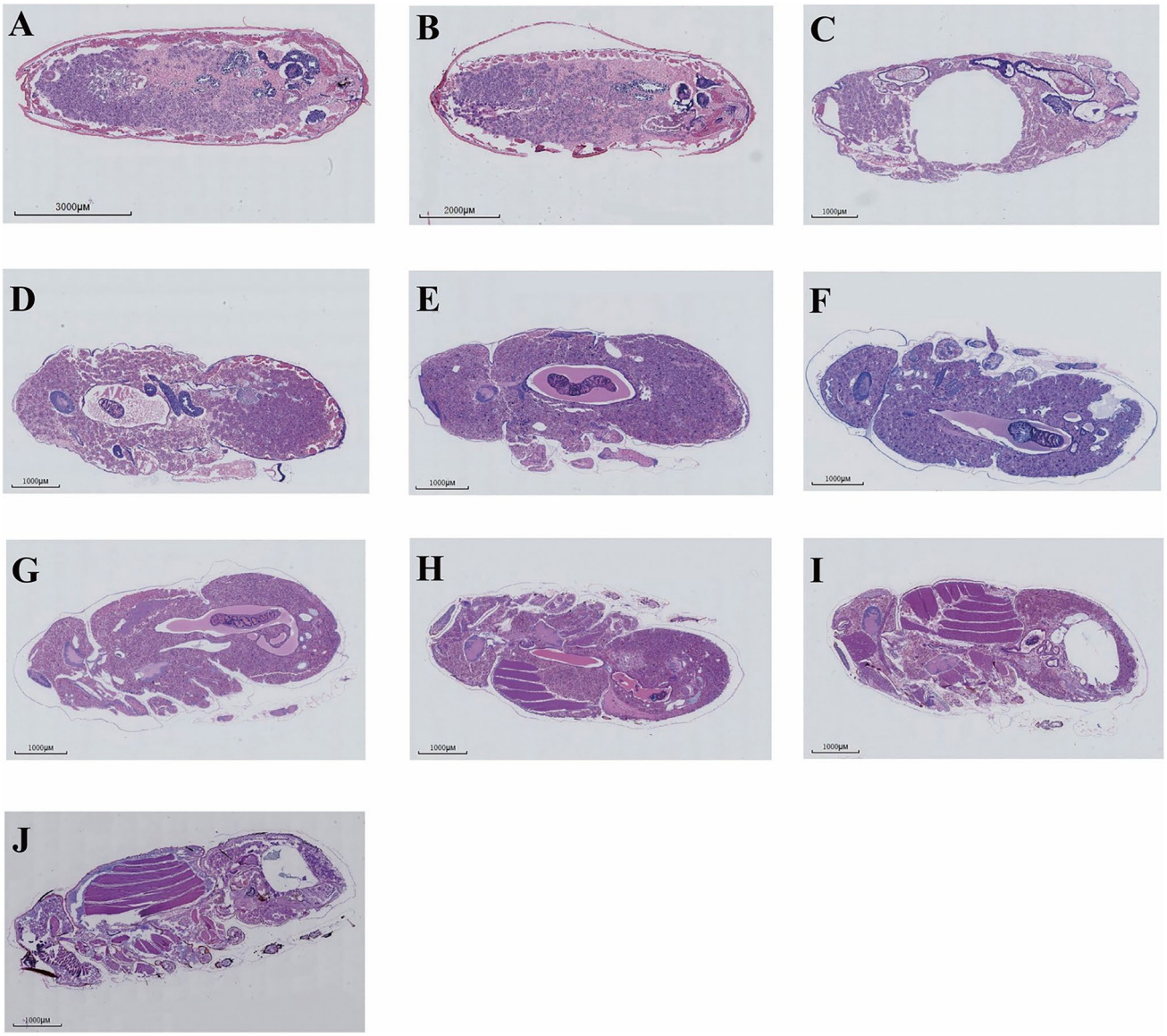

Fig. 6 Intrapuparial histological changes of *Sarcophaga peregrina*. **A** Prepupa stage; **B** puparium separation stage; **C** gas bubble stage; **D** yellow body formation stage; **E** Head, thorax, and abdomen clearly delimited stage; **F** pupal–adult apolysis stage; **G** thoracic ganglion and antennae stage; **H** the dilator muscle of the pharynx and gonads obvious stage; **I** the rectal pouch obvious stage; **J** pre-adult stage

at 25 °C. Additionally, we estimated pupal age by using external morphological changes and internal histological changes (Fig. 8d, e) and DEGs. We estimated the developmental time of the pupa to be approximately 275–339 h by using the above-mentioned methods. PMI_{min} was estimated to be approximately 263–327 h, after subtracting the time between sampling and analyzing (12 h). The detailed estimation results are shown in Table 8. With respect to the case, a surveillance video showed that the woman returned to the rented room at 2000 on May 9, 2020, and did not leave again. Therefore, the PMI was close to 305 h, which is within our estimated range for the time of death.

Discussion

Forensic entomology has become an increasingly important aspect of forensic science [35], especially with respect to PMI_{min} estimation [36]. However, accurate developmental data of necrophagous insect species are essential for the estimation of PMI_{min} [37]. *Sarcophaga peregrina* is an important necrophagous flesh fly species for forensic investigations. In this study, the growth and development of *S. peregrina* were investigated at constant temperatures between 15 and 35 °C, confirming previous conclusions that the developmental time decreases with increasing temperature [26]. In addition, we found that *S. peregrina* could

Table 6 Intrapuparial development of *S. peregrina* related to hours (h) after pupariation at different temperatures

Sub-stage	15℃				20℃				25℃				30℃			
	Min (h)	Max (h)	Mean	SD	Min (h)	Max (h)	Mean	SD	Min (h)	Max (h)	Mean	SD	Min (h)	Max (h)	Mean	SD
A	0	24	13.89	11.85	0	16	9.93	6.18	0	8	5.47	3.72	0	8	4.57	3.96
B	24	48	34.67	11.93	16	40	27.29	8.26	8	24	17.23	6.91	8	24	15.38	6.63
C	48	96	73.71	19.17	40	72	57.52	10.94	32	56	43.73	9.18	24	48	35.73	8.70
D	120	192	157.71	26.78	80	112	95.11	10.96	56	80	70.67	8.94	56	72	64.53	6.83
E	192	264	225.23	27.51	112	152	131.64	14.62	88	112	101.05	9.07	72	96	83.50	8.47
F	264	360	310.50	33.37	160	208	183.33	15.48	120	152	137.26	11.39	96	120	110.12	8.90
G	384	480	434.67	33.84	216	240	227.50	8.93	152	184	167.16	11.58	120	136	127.53	6.98
H	480	600	536.40	76.55	240	280	260.95	13.85	192	216	204.21	9.13	144	152	148.89	9.67
I	576	696	633.60	78.58	288	328	308.19	14.10	224	240	232.57	6.39	152	168	156.50	9.37
J	696	792	746.82	67.65	328	376	352.92	16.65	240	256	251.37	8.73	168	184	173.43	6.39

complete development from larva to adult at 15 °C, but not at 35 °C. When compared with other flesh fly species commonly found on human remains (such as *P. similis*), *S. peregrina* showed a longer development period at 25 °C and 30 °C [8] and could therefore be particularly useful in investigating deaths with a longer PMI_{min}. We used the thermal summation model to calculate a D_0 value of 9.6 °C, which is close to 10.87 °C reported in previous studies [26]. We found the pupal development durations of *S. peregrina* at 25 °C and 20 °C were 249.3 h and 364.6 h, respectively; these results differ from those of a previous study: 270.0 h at 25 °C, 490.0 h at 19 °C, and 366.8 h at 22 °C [26]. Temperatures, different geographical regions [38], different populations [39], humidity and photoperiod [40], and tissue type of food consumed [41, 42] are important factors that affect the developmental time of forensically important flies.

Pupae are common entomological evidence at crime scenes, as the pupal stage can account for up to 50% of the developmental time [43] and even 68% in the case of *S. peregrina*. Traditional methods such as length and weight measurements used to determine the age of larvae cannot be applied because the length of a pupa is stable and the weight of a pupa is a very variable factor [44]. Therefore, more advanced methods such as intrapuparial morphological characteristics, histological analysis, and DEGs have been used to estimate the age during the pupal development of forensically important flies [17].

The analysis of external morphological changes of a dissected pupa with a stereomicroscope is a feasible and inexpensive method. On the basis of the separation and color changes of tissues and organs, intrapuparial development is subdivided into a few sub-stages for estimating pupal age [17].

The morphology of a pupa was divided into 4 stages in previous studies: prepupal stage, phanerocephalic pupal stage, cryptocephalic pupal stage, and pharate adult stage [45]. Later studies examined pupation in more detail, and intrapuparial development was further subdivided into phases according to the development of tissues and organs and color changes [46]. These categorizations can be used for rapid pupal age estimation. In this study, we investigated the external morphological characteristics of *S. peregrina* during intrapuparial development by using a stereomicroscope-based method. The characteristics observed in our study were similar to those reported in previous studies [17], and the intrapuparial period was divided into 12 sub-stages on the basis of the overall external morphological changes. Moreover, we studied temporal changes in individual morphological features of *S. peregrina*, including compound eyes, antennae, mouthparts, thorax, abdomen, legs, and wings, and divided the intrapuparial period into 6 sub-stages. We found that each individual's intrapuparial morphological structure can provide a precise age for the pupae. This finding is consistent with that obtained

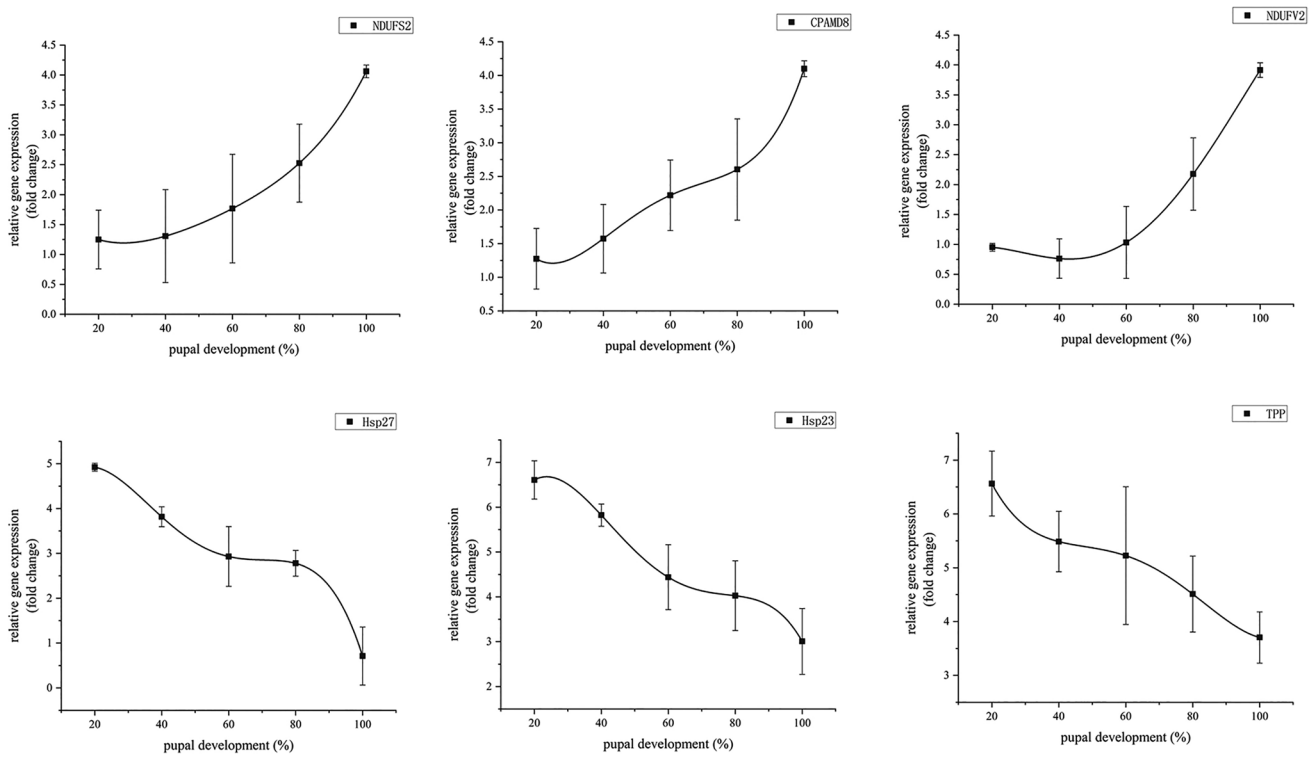

Fig. 7 Differential gene expression levels of *S. peregrina* during intrapuparial development. LogFC values of 6 DEGs at 25° C constant temperature were averaged and plotted against the percentage of intrapuparial development. The data for regression were fit using fourth-order polynomials. The dots represent the mean values. The vertical bars represent the standard deviation

Table 7 The relationship between the relative gene expression (fold change) of *S. peregrine* pupae (y) and the percentage (x) (%) of pupal development at 25 °C constant temperatures

Gene	Simulation equation	Residual sum of squares	R^2 (COD)	*P*
NDUFS2	$y = 2.27739 - 0.09716*x\text{^}1 + 0.00287*x\text{^}2 - 3.22691E\text{-}5*x\text{^}3 + 1.50514E\text{-}7*x\text{^}4$	0	1	< 0.001
CPAMD8	$y = 3.90117 - 0.27236*x\text{^}1 + 0.00916*x\text{^}2 - 1.15635E\text{-}4*x\text{^}3 + 5.15166E\text{-}7*x\text{^}4$	0	1	< 0.001
NDUFV2	$y = 0.48624 + 0.06683*x\text{^}1 - 0.003*x\text{^}2 + 4.49244E\text{-}5*x\text{^}3 - 1.81313E\text{-}7*x\text{^}4$	0	1	< 0.001
Hsp27	$y = 2.56846 + 0.30498*x\text{^}1 - 0.01255*x\text{^}2 + 1.75486E\text{-}4*x\text{^}3 - 8.23855E\text{-}7*x\text{^}4$	0	1	< 0.001
Hsp23	$y = 2.07435 + 0.47765*x\text{^}1 - 0.01616*x\text{^}2 + 1.96737E\text{-}4*x\text{^}3 - 8.20078E\text{-}7*x\text{^}4$	0	1	< 0.001
TPP	$y = 11.35796 - 0.40131*x\text{^}1 + 0.01014*x\text{^}2 - 1.11366E\text{-}4*x\text{^}3 + 4.24612E\text{-}7*\text{x}\text{^}4$	0	1	< 0.001

by Brown et al. [46] and Wang et al. [17]. Furthermore, the 2 processes could complement each other and improve the accuracy of intrapuparial age estimation.

Internal morphological changes can provide clues to the pupal age during metamorphosis by using histological methods. Davies and Harvey [32] and Zajac and Amendt [19] performed histological analysis to determine the age of forensically relevant blow flies during the intrapuparial period. Without histological analysis, it is difficult to determine the completeness of apolysis [17]. We divided the internal morphological changes of *S. peregrina* during the pupal developmental stage into 10 sub-stages on the basis of histological analysis. Additionally, we recorded the time ranges of each sub-stage. We found that the

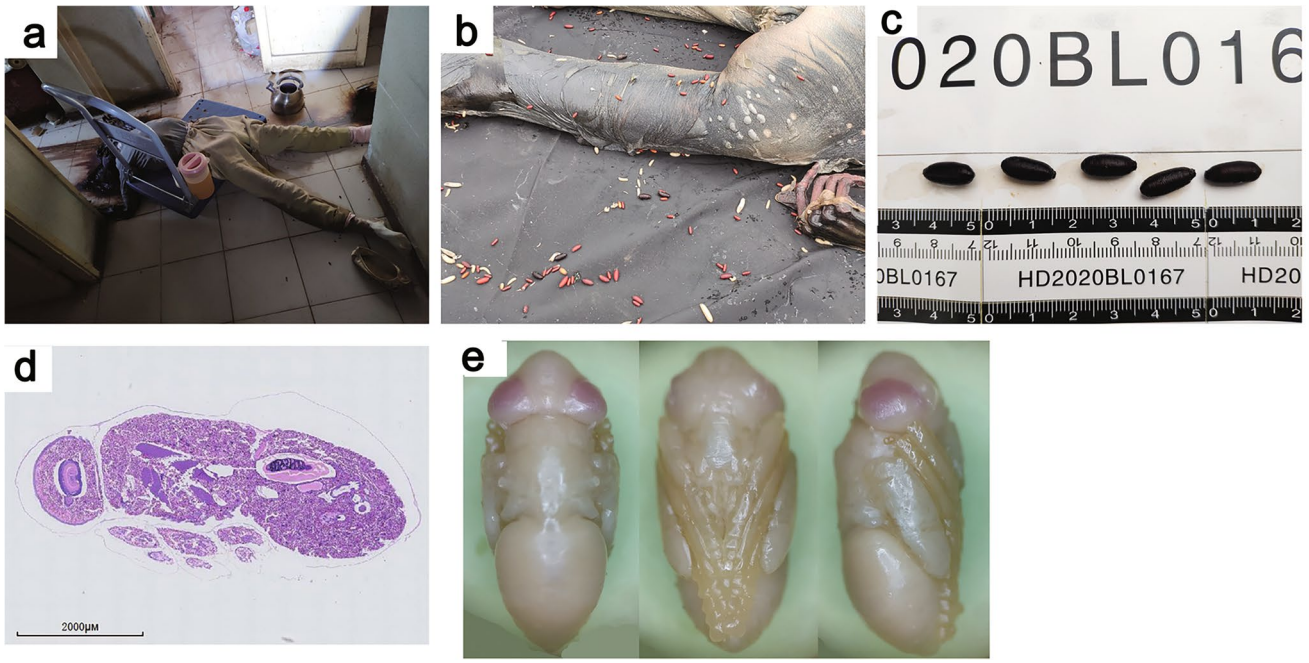

Fig. 8 Case report: **a** scene of death; **b** insect on a corpse; **c** pupae at the death scene; **d** intrapuparial internal histological changes; **e** intrapuparial external morphological changes

Table 8 Case of application of *S. peregrina* in estimation of PMI_{min}

Methods	Indicators	Estimate pupae stage	Estimate pupae time/h	Larval development time/h	Estimate PMImin/h
Development patterns	Developmental events	Pupae stage	0–249	155	155–404
Morphological changes	Overall morphological change	Pink eye stage (G)	144–168		299–323
	Compound eyes	Pink compound eyes (d)	144–168		299–323
	Antenna	Antennae obvious contours (c)	128–176		283–331
	Thorax	Thoracic dorsal bristles with a light yellow color (c)	176–184		331–339
	Abdomen	Abdomen dorsal bristles with a light yellow color (c)	176–184		331–339
	Legs	Light brown legs (d)	176–200		331–355
	Wings	Thin wings, with visible veins (c)	80–176		235–331
Histological analysis	Internal histology Changes	Pupal–adult apolysis stage (F)	120–152		275–307
Differential gene expression	NDUFS2	45% percentage of intra-puparial	112		267
	CPAMD8	63% percentage of intra-puparial	157		312
	NDUFV2	74% percentage of intra-puparial	184		339
	Hsp27	68% percentage of intra-puparial	169		324
	Hsp23	57% percentage of intra-puparial	142		297
	TPP	65% percentage of intra-puparial	162		317
Comprehensive estimate development time of samples			120–184	155	275–339
Actual PMI					305

HE-stained pupal sections revealed different changes in the tissues and organs, such as gas bubble, yellow body, midgut, thoracic ganglion, and dorsal longitudinal muscle, throughout the pupal stage, which provided additional development information and the potential for age estimation during the intrapuparial period. In addition, we found that these characteristics of morphological changes of the newly forming fly in the pupa are similar in many forensically important flies, including the external morphological changes and internal histologic changes [16, 17]. But due to the time of pupa development varies between different fly species [9, 26], the time ranges of each morphological features are inconsistent across fly species. Thus, it is necessary to determine the time ranges of these morphological features in more necrophagous flies species for estimating the PMImin.

The morphological changes of the pupa within the puparium are inconspicuous during the intermediate period; however, the expression of target genes is regular and reliable, providing additional clarity for accurate intrapuparial age estimation. Several studies have shown that the analysis of DEGs could be used for the age estimation of forensically important blow flies such as *Lucilia sericata* (by genes *bcd*, *sll*, and *cs* [12] and genes *ace*, *cs*, *hsp90*, *hsp60*, *ecr*, *rop-1*, *w*, *usp*, and *sll*) [20]), *Calliphora vicina* (by genes *15_2*, *2,014,192*, *actin*, and *arylphorin receptor* [47] and genes *hsp23*, *hsp24*, and *hsp70* [48]), *Lucilia illustris* (by genes *actin*, *15_2*, and *tbp* [17]), and *Chrysomya albiceps* (by genes *Hsp90*, *EcdR* and *2,014,192* [49]) and flesh flies *Sarcophaga dux* (by genes *Hsp60*, *A-alpha*, *ARP* and *RPL8* [9]) and *S. peregrina* (by genes *Hsp90*, *A-alpha*, *AFP*, and *AFBP* [23]). In addition, Hartmann et al. (2021) found that the genetic landmarks showed uniform expression patterns during the metamorphosis of *Calliphora vicina* pupae under constant and fluctuating temperatures [50].

The ideal DEGs for determining insect age should display a steady increase or decrease in expression levels throughout the intrapuparial stage, with each relative expression level corresponding to a specific developmental period. During fly metamorphosis, the transcriptome database allows for more effective selection of appropriate markers to design specific assays for estimating pupal age on the basis of gene expression analysis [58]. In the present study, we selected 6 DEGs from the transcriptomes of different pupal developmental stages of *S. peregrina*, and the expression levels exhibited a steady increase or decrease for the estimation of age during the intrapuparial phase. The results indicated that these DEGs have the potential to estimate the pupal age of *S. peregrina*.

Ying et al. (2013) estimated the PMI of a decomposing corpse was between 90 and 120 h on the basis of the larval length of *S. peregrina*. However, according to the forensic investigation, the PMI was inaccurately estimated [24]. In this study, we estimated the pupal development time of samples from the death scene and body by using morphological features, histological changes, and DEGs and combined them with the larval development time, and we were able to successfully estimate PMI_{min} by combining several methods. Therefore, a combination of various approaches, basic developmental data, external morphological changes, histological analysis, and gene expression profiles, could potentially yield a more precise PMI_{min}.

Supplementary Information The online version contains supplementary material available at https://doi.org/10.1007/s00414-022-02934-7.

Acknowledgements We thank Prof. Lushi Chen (Guizhou Police Officer Vocational College) for his assistance with identification of insects.

Author contribution All authors contributed to the study conception and design. Yanjie Shang, Lipin Ren, Fengqin Yang, and Xiangyan Zhang performed material preparation, data collection, and analysis. Yanjie Shang wrote the first draft of the manuscript. Jens Amendt, and Yu Wang commented on previous versions of the manuscript. Changquan Zhang and Yadong Guo supervised the project. All authors read and approved the final manuscript.

Funding This work was supported by grants from the National Natural Science Foundation of China (grant number 82072114); the Natural Science Foundation of Changsha, China (grant number kq2202129); and the Fundamental Research Funds for the Central Universities of Central South University (grant number 2021zzts0311).

Data availability Not applicable.

Code availability Not applicable.

Declarations

Research involving human participants and/or animals Not applicable.

Ethics approval Not applicable.

Consent to participate Not applicable.

Consent for publication Not applicable.

Conflict of interest The authors declare no competing interests.

References

1. Amendt J, Campobasso CP, Gaudry E, Reiter C, LeBlanc HN, Hall MJR (2007) Best practice in forensic entomology—standards and guidelines. Int J Legal Med 121:90–104
2. Amendt J, Richards CS, Campobasso CP, Zehner R, Hall MJR (2011) Forensic entomology: applications and limitations. Forensic Sci Med Pathol 7:379–392
3. Amendt J (2018) Forensic entomology. Forensic Sci Res 3:1
4. Ren L, Shang Y, Chen W, Meng F, Cai J, Zhu G, Chen L, Wang Y, Deng J, Guo Y (2018) A brief review of forensically important flesh flies (Diptera: Sarcophagidae). Forensic Sci Res 3:16–26

5. Vasconcelos SD, Soares TF, Costa DL (2014) Multiple colonization of a cadaver by insects in an indoor environment: first record of Fannia trimaculata (Diptera: Fanniidae) and Peckia (Peckia) chrysostoma (Sarcophagidae) as colonizers of a human corpse. Int J Legal Med 128:229–233
6. Pohjoismaki JL, Karhunen PJ, Goebeler S, Saukko P, Saaksjarvi IE (2010) Indoors forensic entomology: colonization of human remains in closed environments by specific species of sarcosaprophagous flies. Forensic Sci Int 199:38–42
7. Cherix D, Wyss C, Pape T (2012) Occurrences of flesh flies (Diptera: Sarcophagidae) on human cadavers in Switzerland, and their importance as forensic indicators. Forensic Sci Int 220:158–163
8. Yang L, Wang Y, Li L, Wang J, Wang M, Zhang Y, Chu J, Liu K, Hou Y, Tao L (2017) Temperature-dependent development of Parasarcophaga similis (Meade 1876) and its significance in estimating postmortem interval. J Forensic Sci 62:1234–1243
9. Zhang X, Li Y, Shang Y, Ren L, Chen W, Wang S, Guo Y (2020) Development of Sarcophaga dux (Diptera: Sarcophagidae) at constant temperatures and differential gene expression for age estimation of the pupae. J Therm Biol 93:102735
10. Amoudi MA, Diab FM, Abou-Fannah SS (1994) Development rate and mortality of immature Parasarcophaga (Liopygia) ruficornis (Diptera: Sarcophagidae) at constant laboratory temperatures. J Med Entomol 31:168–170
11. Wang Y, Hu G, Zhang Y, Wang M, Amendt J, Wang J (2019) Development of Muscina stabulans at constant temperatures with implications for minimum postmortem interval estimation. Forensic Sci Int 298:71–79
12. Boehme P, Spahn P, Amendt J, Zehner R (2013) Differential gene expression during metamorphosis: a promising approach for age estimation of forensically important Calliphora vicina pupae (Diptera: Calliphoridae). Int J Legal Med 127:243–249
13. Brown K, Harvey M (2014) Optical coherence tomography: age estimation of Calliphora vicina pupae in vivo? Forensic Sci Int 242:157–161
14. Martin-Vega D, Simonsen TJ, Wicklein M, Hall M (2017) Age estimation during the blow fly intra-puparial period: a qualitative and quantitative approach using micro-computed tomography. Int J Legal Med 131:1429–1448
15. Voss SC, Magni P, Dadour I, Nansen C (2017) Reflectance-based determination of age and species of blowfly puparia. Int J Legal Med 131:263–274
16. Wang Y, Hou Y, Wang M, Wang Y, Xu W, Zhang Y, Wang J (2022) Intrapuparial development and age estimation of Calliphora grahami (Diptera: Calliphoridae) for postmortem interval estimation. J Med Entomol 59:454–466
17. Wang Y, Gu ZY, Xia SX, Wang JF, Zhang YN, Tao LY (2018) Estimating the age of Lucilia illustris during the intrapuparial period using two approaches: Morphological changes and differential gene expression. Forensic Sci Int 287:1–11
18. Salazar-Souza M, Couri MS, Aguiar VM (2018) Chronology of the intrapuparial development of the blowfly Chrysomya albiceps (Diptera: Calliphoridae): application in forensic entomology. J Med Entomol 55:825–832
19. Tarone AM, Jennings KC, Foran DR (2007) Aging blow fly eggs using gene expression: a feasibility study. J Forensic Sci 52:1350–1354
20. Tarone AM, Foran DR (2011) Gene expression during blow fly development: improving the precision of age estimates in forensic entomology. J Forensic Sci 56(Suppl 1):S112–S122
21. Boehme P, Spahn P, Amendt J, Zehner R (2014) The analysis of temporal gene expression to estimate the age of forensically important blow fly pupae: results from three blind studies. Int J Legal Med 128:565–573
22. Ren L, Shang Y, Yang L, Wang S, Wang X, Chen S, Bao Z, An D, Meng F, Cai J, Guo Y (2020) Chromosome-level de novo genome assembly of Sarcophaga peregrina provides insights into the evolutionary adaptation of flesh flies. Mol Ecol Resour
23. Shang Y, Ren L, Yang L, Wang S, Chen W, Dong J, Ma H, Qi X, Guo Y (2020) Differential gene expression for age estimation of forensically important Sarcophaga peregrina (Diptera: Sarcophagidae) intrapuparial. J Med Entomol 57:65–77
24. Ying L, Chen Y, Guo Y, Lagabaiyila Z, Li L (2013) Estimation of post-mortem interval for a drowning case by using flies (Diptera) in Central-South China: implications for forensic entomology. Rom J Leg Med 21:293–298
25. Wang Y, Wang J, Wang Z, Tao L (2017) Insect succession on pig carcasses using different exposure time - a preliminary study in Guangzhou, China. J Forensic Leg Med 52:24–29
26. Wang Y, Wang JF, Zhang YN, Tao LY, Wang M (2017) Forensically important Boettcherisca peregrina (Diptera: Sarcophagidae) in China: development pattern and significance for estimating postmortem interval. J Med Entomol 54:1491–1497
27. Zhang Y, Wang Y, Yang L, Tao L, Wang J (2018) Development of Chrysomya megacephala at constant temperatures within its colony range in Yangtze River Delta region of China. Forensic Sci Res 3:74–82
28. Bambaradeniya YTB, Karunaratne WAIP, Tomberlin JK, Magni PA (2021) Effect of type of tissue on the development of Chrysomya rufifacies (Diptera: Calliphoridae) in Sri Lanka. J Med Entomol 58:1673–1679
29. Chen LS: Necrophagous flies in China. Guizhou Sci Technol Press, Guiyang, China..
30. Bugelli V, Campobasso CP, Verhoff MA, Amendt J (2017) Effects of different storage and measuring methods on larval length values for the blow flies (Diptera: Calliphoridae) Lucilia sericata and Calliphora vicina. Sci Justice 57:159–164
31. Lecheta MC, Moura MO (2019) Estimating the age of forensically useful blowfly, Sarconesia chlorogaster (Diptera: Calliphoridae), using larval length and weight. J Med Entomol 56:915–920
32. Ren L, Shang Y, Yang L, Wang S, Wang X, Chen S, Bao Z, An D, Meng F, Cai J, Guo Y (2021) Chromosome-level de novo genome assembly of Sarcophaga peregrina provides insights into the evolutionary adaptation of flesh flies. Mol Ecol Resour 21:251–262
33. Ikemoto T, Takai K (2000) A new linearized formula for the law of total effective temperature and the evaluation of line-fitting methods with both variables subject to error. Environ Entomol 29:671–682
34. Wang Y, Zhang Y, Wang M, Hu G, Fu Y, Zhi R, Wang J (2021) Development of Hydrotaea spinigera (Diptera: Muscidae) at constant temperatures and its significance for estimating postmortem interval. J Med Entomol 58:56–63
35. Wang M, Chu J, Wang Y, Li F, Liao M, Shi H, Zhang Y, Hu G, Wang J (2019) Forensic entomology application in China: four case reports. J Forensic Leg Med 63:40–47
36. Acosta X, Gonzalez-Reyes AX, Corronca JA, Centeno ND (2021) Estimation of the postmortem interval through the use of development time of two South American species of forensic importance of the genus Lucilia (Diptera: Calliphoridae). J Med Entomol 58:1064–1073
37. Wang M, Wang Y, Hu G, Wang Y, Xu W, Wu M, Wang J (2020) Development of Lucilia sericata (Diptera: Calliphoridae) under constant temperatures and its significance for the estimation of time of death. J Med Entomol 57:1373–1381
38. Tarone AM, Picard CJ, Spiegelman C, Foran DR (2011) Population and temperature effects on Lucilia sericata (Diptera: Calliphoridae) body size and minimum development time. J Med Entomol 48:1062–1068

39. Nabity PD, Higley LG, Heng-Moss TM (2007) Light-induced variability in development of forensically important blow fly Phormia regina (Diptera: Calliphoridae). J Med Entomol 44:351–358
40. Bambaradeniya Y, Karunaratne W, Tomberlin JK, Goonerathne I, Kotakadeniya RB, Magni PA (2019) Effect of temperature and tissue type on the development of the forensic fly Chrysomya megacephala (Diptera: Calliphoridae). J Med Entomol 56:1571–1581
41. Bambaradeniya Y, Karunaratne W, Tomberlin JK, Goonerathne I, Kotakadeniya RB (2019) Effect of temperature and tissue type on the development of myiasis causing fly; Chrysomya bezziana (Diptera: Calliphoridae). J Med Entomol 56:625–631
42. Fratczak-Lagiewska K, Grzywacz A, Matuszewski S (2020) Development and validation of forensically useful growth models for Central European population of Creophilus maxillosus L. (Coleoptera: Staphylinidae). Int J Legal Med 134:1531–1545
43. Feng DX, Wu J, Sun DP (2021) Intrapuparial age estimation of forensically important Dohrniphora cornuta (Diptera: Phoridae). J Med Entomol 58:616–624
44. Fraenkel G, Bhaskaran G (1973) Pupariation and pupation in Cyclorrhaphous flies (Diptera): terminology and interpretation. Ann Entomol Soc Am 66:418–422
45. Brown K, Thorne A, Harvey M (2015) Calliphora vicina (Diptera: Calliphoridae) pupae: a timeline of external morphological development and a new age and PMI estimation tool. Int J Legal Med 129:835–850
46. Zajac BK, Amendt J (2012) Bestimmung des Alters forensisch relevanter Fliegenpuppen. Rechtsmedizin 22:456–465
47. Fremdt H, Amendt J, Zehner R (2014) Diapause-specific gene expression in Calliphora vicina (Diptera: Calliphoridae)—a useful diagnostic tool for forensic entomology. Int J Legal Med 128:1001–1011
48. Alajmi R, Alotaibi F, Ahmed A, Alkuriji M, Alrajeh A, Metwally D, Haddadi R, Almeaiweed N, Almutairi B (2021) Gene expression as age estimation marker in the larval stages of the forensic blowfly, Chrysomya albiceps, at different temperatures. J Forensic Leg Med 77:102096
49. Hartmann K, Herrmann E, Amendt J, Verhoff MA, Zehner R (2021) Age-dependent gene expression of Calliphora vicina pupae (Diptera: Calliphoridae) at constant and fluctuating temperatures. Int J Legal Med 135:2625–2635
50. Zajac BK, Amendt J, Horres R, Verhoff MA, Zehner R (2015) De novo transcriptome analysis and highly sensitive digital gene expression profiling of Calliphora vicina (Diptera: Calliphoridae) pupae using MACE (Massive Analysis of cDNA Ends). Forensic Sci Int Genet 15:137–146